The prediction of separation of the turbulent boundary layer

By B. S. STRATFORD
National Gas Turbine Establishment, Farnborough

(Received 17 July 1958)

A rapid method for the prediction of flow separation results from an approximate solution of the equations of motion; a single empirical factor is required. The equations are integrated by a modified 'inner and outer solutions' technique developed recently for laminar boundary layers, the criterion for separation being obtained as a simple formula applying directly to the separation position. At Reynolds numbers of the order of 10^6, the criterion is

$$C_p(x\,dC_p/dx)^{\frac{1}{2}} = 0{\cdot}39(10^{-6}R)^{\frac{1}{10}},$$

when $d^2p/dx^2 \geqslant 0$ and $C_p \leqslant \frac{4}{7}$; the coefficient 0·39 is replaced by 0·35 when $d^2p/dx^2 < 0$.

The prediction of the pressure rise to separation is likely to be from 0 to 10 % too low, which puts it second in accuracy to those methods, such as Maskell's (1951), which utilize the Ludweig–Tillmann skin friction law. However, the convenience of the method makes the present error acceptable for many applications, while a greater accuracy should be attainable from an improved allowance for the quantity d^2p/dx^2.

The main derivation is for arbitrary pressure distributions, while an extension leads to the pressure distribution which just maintains zero skin friction throughout the region of pressure rise.

The concept of a turbulent inner layer with zero wall stress is put forward, and it is deduced that in the neighbourhood of the wall the velocity is proportional to the square root of the distance from the wall.

1. Introduction

Previous methods for calculating the position of separation for the turbulent boundary layer—i.e. the position at which the flow 'stalls' or separates from the wall—have solved the momentum or energy equations in conjunction with empirical expressions representing the shape and behaviour of the velocity profile (see von Doenhoff & Tetervin 1943; Goldstein 1938; Kalikhmann 1943; Rotta 1953; Spence 1956*a*, *b*; Squire & Young 1937; and Maskell 1951). These methods are reasonably accurate, but provide only a limited understanding of the flow.

The present method is based upon the equations of motion (Goldstein 1938), the analysis of the turbulence utilizing either dimensional analysis or mixing length theory (Durand 1943, §25). Moreover, a closer physical picture than

hitherto is attempted for the flow. The method postulates that, as for the laminar layer (Stratford 1954), the turbulent layer in a pressure rise may be divided into two distinct regions. The outer is an historical region in which the pressure rise just causes a lowering of the dynamic head profile, the losses due to the shear

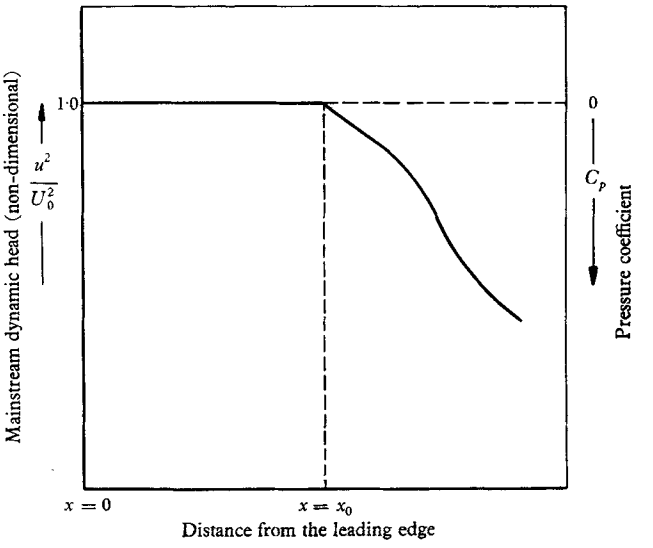

FIGURE 1. The type of pressure distribution treated initially.

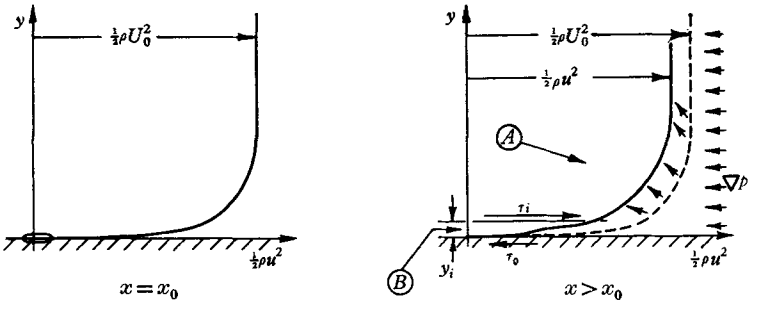

FIGURE 2. Development of a boundary layer in a sudden pressure gradient. At $x = x_0$ the profile is unchanged except at $y = 0$. Just downstream of x_0 there is a general lowering of velocity in the outer layer (A) and a change of shape in the inner layer (B).

stresses being almost the same as for the flow on a flat plate. The general solution is obtained in terms of the flow on a flat plate, the relationship to the flat plate flow being identical with the corresponding relationship for the laminar boundary layer. In the inner layer, on the other hand, the inertia forces are small so that the velocity profile is distorted by the pressure gradient until the latter is largely balanced by the transverse gradient of shear stress. The solution found for the inner layer at the separation position is such that close to the wall the velocity is proportional to the square root of the distance from the wall. This velocity profile is in contrast to that for the laminar boundary layer at separation, where the velocity is proportional to the square of the distance from the wall. A summary of the treatment and a picture of the flow is sketched in figures 1 to 3. It will be seen

from figure 1 that the pressure distribution considered initially has a simplified form in which a sharp pressure rise starts abruptly at the position $x = x_0$ after constant pressure for a distance x_0.

The final solution is given by equations (19*a*), (19*c*) and (23). These relate x, C_p and dC_p/dx at the separation position, and may be applied very rapidly to any given pressure distribution.

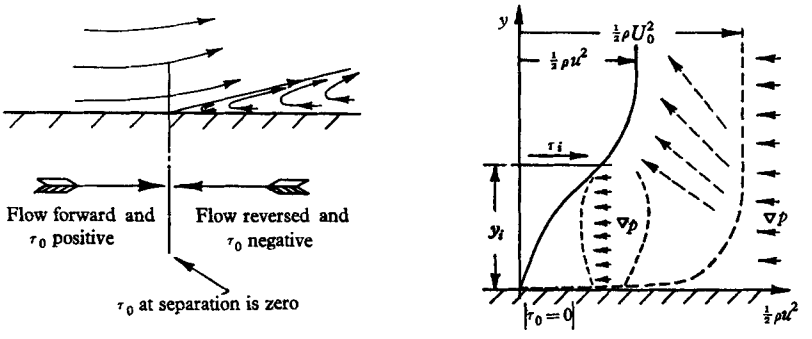

FIGURE 3. The separation position. The flow reaches the separation condition of zero skin friction when the backward force $y_i \nabla p$ can only be adequately balanced by the shear stress difference $(\tau_i - \tau_0)$ if τ_0 is zero.

2. The outer layer

Where there is a rapid pressure rise the shear forces in the outer part of the boundary layer are small compared with either the inertia forces or the pressure gradient. As a preliminary it will be found helpful to consider the solution for a flow in which, downstream of x_0, the shear forces are supposed zero, even though vorticity is present.

In such a flow the total pressure, P, will remain constant along a streamline and Bernoulli's equation holds:

$$\frac{\partial P}{\partial s} = 0 \quad \text{(zero shear stress)},$$

where s is the distance along a streamline. Thus

$$P(x, \psi) = P(x_0, \psi) \quad \text{(zero shear stress)}.$$

The solution is therefore that the dynamic head at any point is equal to the dynamic head on the same streamline at x_0 minus the rise in static pressure. Since the flow at x_0 is known, the flow in the outer region of the boundary layer downstream of x_0 is solved.

For the real flow the shear forces cause a decrease in total pressure along a streamline, Bernoulli's equation being replaced by

$$\frac{\partial P}{\partial s} = \frac{\partial \tau}{\partial y}, \tag{1}$$

as may be deduced from the equations of motion and continuity; τ is the shear stress and y is the distance from the wall. Thus

$$P(x, \psi) = P(x_0, \psi) + \int_{x_0}^{x} \frac{\partial \tau}{\partial y} ds. \tag{2}$$

Let the flow under consideration now be compared with a second flow which has identical conditions as far as $x = x_0$, but which continues at constant static pressure thereafter. The distributions of $\partial\tau/\partial y$ for the two flows will be identical for points away from the wall at $x = x_0$; also the distributions will remain closely the same for a short distance downstream of x_0, because the effect of the pressure rise in the outer part of the boundary layer in this region is to cause a general lowering of the velocity profile rather than a change in shape. It follows, using equation (2), that the total pressure loss caused by the shear forces will be approximately the same for the two flows. Thus the total pressures, which were equal at x_0, may as an approximation still be supposed equal at points just downstream of x_0, i.e.

$$P(x, \psi) = P'(x, \psi) \quad (\psi \geqslant \psi_i), \tag{3}$$

where the dash denotes the comparison profile,

$$\psi = \int_0^y u\, dy,$$

and where the condition $\psi \geqslant \psi_i$ denotes an application limited to the outer region of the profile (ψ_i is the value of ψ at the edge of the inner layer).

Since $p' = \text{constant} = p_0$, where p is the static pressure, equation (3) gives

$$\tfrac{1}{2}\rho u^2(x, \psi) = \tfrac{1}{2}\rho u'^2(x, \psi) - (p - p_0) \quad (\psi \geqslant \psi_i). \tag{4}$$

The dynamic head at any point is therefore equal to the dynamic head at the corresponding point in the comparison flow minus the rise in static pressure.

Equation (4) represents for the outer part of the boundary layer a solution which is almost exact at positions a short distance downstream of x_0 (since the values of both $\frac{1}{2}\rho u^2$ and $(\partial/\partial s)\,\frac{1}{2}\rho u^2$ are exact at x_0), and which would be expected to indicate at least the main behaviour for large distances downstream of x_0. (For an alternative assessment, the reduction in the value of the local dynamic head $\frac{1}{2}\rho u^2$ from its initial value $\frac{1}{2}\rho U_0^2$ may be divided into three parts, these being due respectively to the rise in static pressure, to the viscosity between $x = 0$ and $x = x_0$, and to the viscosity downstream of x_0. Of these three effects, the first two have been included exactly in equation (4). The third effect, which is likely to be relatively small for the outer part of a boundary layer at separation, has been allowed for approximately.)

The standard solution required for u', the velocity in the boundary layer without pressure rise, may for the turbulent boundary layer be taken as the following semi-empirical form. (The usual derivation is that given by Goldstein (1938), while Schlichting (1941) obtains the result by approximate solution of the equations of motion.)

$$\frac{u'}{U_0} = \left(\frac{y'}{\delta'}\right)^{1/n}, \tag{5a}$$

where

$$\delta' = \frac{(n+1)\,(n+2)}{n}\,\theta', \tag{5b}$$

$$\theta' = 0{\cdot}036 x R^{-\frac{1}{5}}, \tag{5c}$$

and where the value of n varies slightly with the Reynolds number but is usually close to 7.

Equations (4) and (5) provide a general solution for the outer region of the boundary layer.

Differentiation of equation (4) with respect to ψ, and replacing $u(\partial/\partial\psi)$ by $\partial/\partial y$, gives

$$\left[\frac{\partial u}{\partial y}\right]_{(x,\psi)} = \left[\frac{\partial u'}{\partial y'}\right]_{(x,\psi)} \quad (\psi \geqslant \psi_i). \tag{6}$$

3. The inner layer

The action of the pressure rise in the outer layer has been interpreted as a direct reduction in the dynamic head along each streamline, the only effect of the shear forces being to cause a superposed, and almost independent, loss. It can therefore be said that in the outer layer the back pressure force is balanced by the fluid inertia forces.

In the inner layer the effect of the fluid inertia is too small for the above mechanism to be possible. In particular the inertial forces at the wall are zero, so that the pressure forces must be balanced entirely by the gradient of the shear force, i.e.

$$\frac{\partial p}{\partial x} = \frac{\partial \tau}{\partial y} \quad (y = 0), \tag{7}$$

as follows from the equations of motion, or from equation (1), by putting $\partial u/\partial s = 0$. Now this balance at the wall can occur only after there has been a change in the profile shape. When the sudden pressure gradient is reached at $x = x_0$, the dynamic head and hence the general level of velocity would start to fall everywhere, were it not for the no slip condition at the wall. This, as it were, anchors the velocity profile, which distorts instantaneously at $x = x_0$, $y = 0$, until, just at the wall, the required balance is attained. The inner layer commences its growth at the discontinuity at $x = x_0$, $y = 0$ and is the region in which the slope of the velocity profile has changed. In the inner layer there is a transition between fluid at the wall, for which the pressure force is balanced entirely by the shear force gradient, and fluid in the outer layer, where the pressure force causes simply a direct reduction of dynamic head.

The analysis may proceed either on dimensional arguments* or by mixing length theory. Using dimensional arguments, suppose we have a layer within which the motion is determined by energy transport due to working by shear stresses, there being relatively little effect from energy advection by the mean flow. The motion then depends on

$$\tau_0, \quad (\partial\tau/\partial y)_0, \quad (\partial^2\tau/\partial y^2)_0,$$

and the kinematic viscosity. If the wall stress, τ_0, is zero, dimensional similarity requires that

$$u = \left(\frac{\nu}{\rho}\frac{\partial\tau}{\partial y}\right)^{\frac{1}{3}} F\left(\frac{1}{\rho}\left(\frac{\partial\tau}{\partial y}\right)_0 \frac{y^3}{\nu^2}\right) \tag{8}$$

sufficiently close to the wall to satisfy $y(\partial^2\tau/\partial y^2)_0 \ll (\partial\tau/\partial y)_0$. In the fully turbulent part of the flow, the relative motion is independent of the viscosity and so

$$u = A\left(\frac{y}{\rho}\frac{\partial\tau}{\partial y}\right)^{\frac{1}{2}} + B\left(\frac{\nu}{\rho}\frac{\partial\tau}{\partial y}\right)^{\frac{1}{3}}, \tag{9}$$

* These were suggested by the referee.

where A, B are absolute constants. For large values of $\left(\frac{1}{\rho}\frac{\partial\tau}{\partial y}\frac{y^3}{\nu^2}\right)$, (9) is nearly

$$\tfrac{1}{2}\rho u^2 = \tfrac{1}{2}A^2 y(\partial\tau/\partial y)_0 = \tfrac{1}{2}A^2 y\,\partial p/\partial x. \tag{10}$$

The alternative analysis by mixing length theory is able to indicate the order of magnitude of the constant of proportionality. The momentum transfer hypothesis will be adopted and, as is conventionally assumed for the flow on a flat plate, the mixing length will as a first approximation be assumed proportional to the distance from the wall. Now by the standard theory (e.g. Durand 1943, § 25) the shear stress when $\partial u/\partial y$ is positive is

$$\tau = \rho K^2 y^2 (\partial u/\partial y)^2 \quad (y \text{ small}), \tag{11}$$

where K is the Karman constant. The boundary layer at separation has zero skin friction, so that the integration of equation (7), regarding this equation as holding over a small region close to the wall, gives

$$\tau = y\,\partial p/\partial x \quad (\tau_0 = 0,\ y \text{ small}). \tag{12}$$

Elimination of τ between equations (11) and (12) yields

$$\left(\frac{\partial u}{\partial y}\right) = \left(\frac{1}{\rho K^2}\frac{\partial p}{\partial x}\right)^{\frac{1}{2}} y^{-\frac{1}{2}} \quad (\tau_0 = 0, y \text{ small}), \tag{13}$$

while for no slip at the wall, $u = 0$ at $y = 0$, and equation (13) integrates to

$$u = \left(\frac{4}{\rho K^2}\frac{\partial p}{\partial x}\right)^{\frac{1}{2}} y^{\frac{1}{2}} \quad (\tau_0 = 0, y \text{ small}), \tag{14}$$

which is in agreement with equation (10).

Thus close to the wall the asymptotic form of the separation profile is that the velocity is proportional to $y^{\frac{1}{2}}$ and the dynamic head is proportional to y.

Equation (14), with an appropriate value for K, could be regarded as the first term of a series expansion representing the whole inner layer profile, the higher terms arising from the inertial forces and the gradual fall-off of the mixing length from the linear value assumed for it. Since the details of the mixing length behaviour could be determined only by recourse to experiment, it is particularly expedient for the present purpose, of calculating the separation position, to incorporate a single empirical factor, say 'β', in this first term, omitting higher terms whatever their source, and to obtain the factor from a special experiment. By omitting the higher terms in the profile expansion the profile has been over-idealized as regards its own shape, so that good agreement with experimental profiles would not be expected, but the empirical factor might be expected adequately to represent the effect on the separation criterion of the higher terms. The factor β will be used also to represent any effects which the pressure rise might have on the mixing length, effects which are discussed in more detail by Ludweig & Tillmann (1949), by Squire (1950), and by Stratford (1956, 1959).

For present purposes, therefore, the inner layer ($y < y_i$) is represented by the idealized profile

$$\tfrac{1}{2}\rho u^2 = \frac{2}{(0{\cdot}41\beta)^2}\frac{\partial p}{\partial x}y \quad (\tau_0 = 0,\ y < y_i), \tag{15}$$

0·41 being the flat plate value for the Karman constant.

Incidentally, the fact that $\partial\tau/\partial y > 0$ and $\partial^2 u/\partial y^2 < 0$ in this flow renders the vorticity transfer theory inapplicable.

4. The joining condition, and the preliminary result

At the join between the inner and outer layers continuity is specified in ψ, u and $\partial u/\partial y$. This is sufficient to determine the join, and the suggested algebra for so doing and for deriving the separation condition (equation 19a) is as follows.

At the join ψ and $\partial u/\partial y$ for the inner layer are equal to ψ and $\partial u/\partial y$ for the outer layer and, therefore, from the definition of corresponding points and from equation (6), ψ and $\partial u/\partial y$ for the inner layer at the join are equal to ψ (or ψ') and $\partial u'/\partial y'$ for the corresponding point on the comparison profile. Equating $\psi(\partial u/\partial y)^3$ and $\psi'(\partial u'/\partial y')^3$, calculated respectively from equations (15) and (5a), gives that the join at the separation position is such that its corresponding point satisfies

$$\left(\frac{y'}{\delta'}\right)^{(2n-4)/n} = \frac{3(0{\cdot}41\beta)^4}{(n+1)\,(n\delta'\,dC_p/dx)^2} \quad (\psi = \psi_i), \tag{16}$$

the join being thus determined. A further property of the join

$$u^2/u'^2 = 3/(n+1) \quad (\psi = \psi_i) \tag{17}$$

is obtained by comparing $u^2/(\psi\,\partial u/\partial y)$, calculated from equation (15), with the corresponding quantity calculated from equation (5a).

The separation condition may now be derived from equation (4) for, from that equation and equation (5a),

$$C_p = (y'/\delta')^{2/n}\,(1 - u^2/u'^2) \quad (\psi \geqslant \psi_i,\ C_p \leqslant [1 - u^2/u'^2]), \tag{18}$$

where $C_p = (p - p_0)/\tfrac{1}{2}\rho U_0^2$. Use of values at the join, as given by equations (16) and (17), followed by substitution of equations (5b) and (5c) for δ', leads to

$$(2C_p)^{\frac{1}{4}(n-2)}\left(x\frac{dC_p}{dx}\right)^{\frac{1}{2}} = 1{\cdot}06\beta(10^{-6}R)^{\frac{1}{10}} \quad \left(C_p \leqslant \frac{n-2}{n+1}\right), \tag{19a}$$

R being the Reynolds number based on the local value of the distance x and the peak velocity U_0. In obtaining equation (19a) the quantity

$$(n+1)^{\frac{1}{4}(n+1)}\,(n+2)^{\frac{1}{2}}/(n-2)^{\frac{1}{4}(n-2)}$$

has been replaced by $10{\cdot}7 \times (2{\cdot}00)^{\frac{1}{4}(n-2)}$, which is within 1 % of the former quantity when $6 \leqslant n \leqslant 8$.

The limitation $C_p \leqslant (n-2)/(n+1)$ results formally from the join of the inner layer with the outer layer reaching the edge of the boundary layer when using the idealized velocity profiles. The same limitation applies to the range over which β has been determined empirically.

The parameter β may be determined by comparison with the experiment which is described in the following paper (Stratford 1959). In this experiment the flow was maintained just at the separation condition throughout the pressure rise, as will be considered theoretically in the last section of the present paper. It is found that β is independent of C_p and has the value

$$\beta = 0{\cdot}66 \quad (\tau_0 \equiv 0,\ C_p \leqslant [n-2]/[n+1]). \tag{19b}$$

The qualification '$\tau_0 \equiv 0$' has been added because β will vary somewhat with the value of d^2p/dx^2 immediately prior to separation, this quantity having its greatest possible negative value in the experiment. The variation will be discussed in §5.

The quantity 'n' pertains to the flat plate comparison profile at $x = x_s$, suffix s being used to denote separation; the relevant Reynolds number is still

$$R_s = x_s U_0/\nu.$$

Now if $C_{p,s} = 0{\cdot}50$ equation (19a) is seen to be independent of n. Moreover, in general it is not sensitive to n, for example, a typical change from $n = 6$ to $n = 7$ has a 4% effect, and so the use of a reasonable value for n is sufficient. Analysis of a velocity profile obtained by Schubauer & Klebanoff (1950) suggests the value $n = 7$ at a Reynolds number of $1{\cdot}43 \times 10^7$, while as part of the experiment with continuously zero skin friction the value $n = 6$ was obtained for a Reynolds number of $0{\cdot}64 \times 10^6$. Comparison of the values of n with those of $\log_{10} R$ and consideration of the degree of accuracy required therefore suggests the use of

$$n = \log_{10} R_s, \tag{19c}$$

the errors thus introduced into the formula being expected to be usually less than 1%.

Except for the small effect of $(d^2p/dx^2)_s$, which will be discussed in §5, equations (19a) to (19c) are sufficient to determine whether separation will occur at any chosen point on a given pressure distribution. This is the principal result of the paper.

Some typical values, and comparison with the laminar boundary layer

Equations (19) demonstrate that the value of the pressure rise to separation is not highly sensitive to the value of the pressure gradient at separation. As a typical example, for a separating turbulent boundary layer the value of $x\,dC_p/dx$ is in the neighbourhood of unity and so the value of C_p at separation would be about 0·35, say between 0·3 and 0·5.

These results are to be compared with results for the laminar layer, which, according to Stratford's (1954) analysis, satisfies

$$C_p\left(x\frac{dC_p}{dx}\right)^2 \doteqdot 0{\cdot}0076 \quad \text{(laminar separation)}.$$

The pressure recovery of the laminar layer at separation is thus much more sensitive to pressure gradient. Values for $(x\,dC_p/dx)_s$ for a laminar boundary layer would usually range between 0·2 and 0·5, or higher, so that a typical pressure recovery is, say, 0·06.

Allowance for an initial region of favourable pressure gradient or laminar flow

For pressure distributions having an initial region of favourable pressure gradient, the value of x to be used in the above equations has to be an equivalent value, the flow with favourable gradient being replaced by one at constant pressure and with a mainstream velocity equal to the peak mainstream velocity U_0. The criterion of equivalence is the value of the boundary layer momentum thickness θ at the point of peak velocity. It may be shown semi-empirically (using the energy equation and the data of Schubauer & Klebanoff (1950)) that for a boundary layer turbulent from the leading edge this criterion leads approximately to

$$x_0 = \int_0^{X_0} \left(\frac{U}{U_0}\right)^3 dX, \tag{20}$$

where X and x are distances from the actual and the equivalent leading edges respectively.

For a boundary layer which is initially laminar the momentum thickness θ_1 at $X = X_1$ may be calculated from the following equation, which has been obtained with minor variations by Young & Winterbottom (1940), Walz (1943) and Thwaites (1949):

$$\theta_1 = 0{\cdot}664\left[\frac{\nu}{U_1}\int_0^{X_1}\left(\frac{U}{U_1}\right)^5 dX\right]^{\frac{1}{2}}. \tag{21}$$

The equivalent length of turbulent boundary layer can now be determined from equation (5*c*) on the standard assumptions of sudden transition and of conservation of momentum. For the final equivalent condition, in which both the boundary layer is entirely turbulent and the pressure is constant at p_0 until the rise of pressure commences, equations (5*c*), (20) and (21) lead to

$$x_0 = 38{\cdot}2\left(\frac{\nu}{X_t U_t}\right)^{\frac{3}{8}}\left(\frac{U_0}{U_t}\right)^{\frac{1}{8}}\left[\int_0^{X_t}\left(\frac{U}{U_0}\right)^5 d\left(\frac{X}{X_t}\right)\right]^{\frac{5}{8}} X_t + \int_{X_t}^{X_0}\left(\frac{U}{U_0}\right)^3 dX, \tag{22}$$

where X is the distance from the actual leading edge and suffix t indicates values at transition. Suffix 0 now refers to conditions at the position of peak velocity, or at transition, whichever is later. If, however, transition is immediately followed by a steep pressure rise leading to separation the present theory would only be roughly correct, as the turbulent flat plate profile assumed to exist at $x = x_0$ would not be properly formed.

The profiles at separation

The derivation of the preceding sections can be used to obtain the profiles at the separation position; these are shown in figure 4 in the form of dynamic head profiles. It will be noticed that there is an appreciable variation in the shape of the separation profile with variation in the value of $C_{p,s}$.

The value of the ratio θ_s/θ', where θ' is the momentum thickness of the comparison boundary layer, is plotted in figure 5 as a function of $C_{p,s}$. The absolute value of θ_s for any given pressure distribution may be found by using this figure together with the relation for θ' from equation (5*c*).

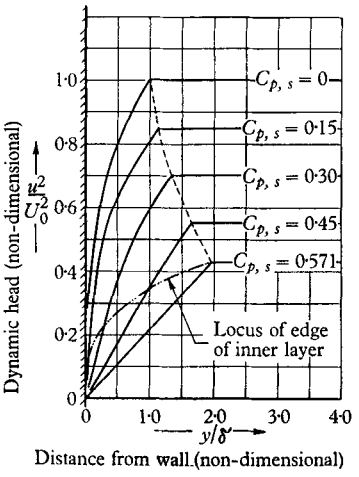

FIGURE 4. The idealized theoretical dynamic head profiles at separation, $R_s = 10^6$, δ' = thickness of the flat plate comparison profile.

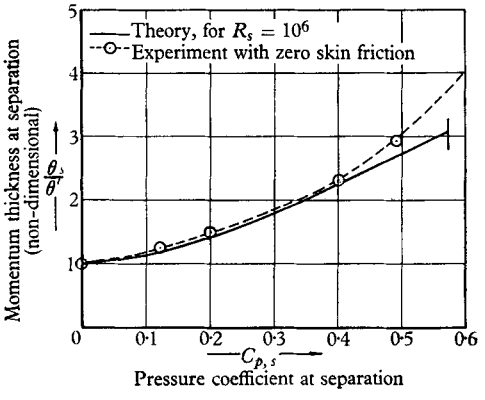

FIGURE 5. Momentum thickness of the boundary layer at separation, θ' = momentum thickness of the comparison profile.

5. Tests of the method and development of the formula to allow for variation of $(d^2p/d^2x)_s$

The formulae (19), of which formula (19*b*) strictly holds only for large negative values of d^2p/dx^2, will be applied to certain test pressure distributions and then a correction discussed for d^2p/dx^2.

The data are taken from von Doenhoff & Tetervin (1943) for the first three tests and from Schubauer & Klebanoff (1950) for the fourth; Schubauer & Klebanoff's measurements were made on a special surface in a large wind tunnel. In order to assist the assessment the experiment used for the empirical determination of β has been included as 'Test' 5. It should be noted that the experimental pressure distributions allow some range of interpretation as regards dp/dx, especially in the neighbourhood of a point of inflexion, and the effect on the theoretical prediction could be as much as $\pm 5\,\%$.

The results are shown in figures 6 and 7 and table 1 (pages 11–13).

It will be seen that in the main tests the prediction for the pressure recovery at separation is always too low. The discrepancy in β varies between 0 and 20%; the discrepancy in $C_{p,s}$ is also in this range, but the precise value depends on how long the boundary layer 'hovers' (due to its softening of the pressure gradient) just close to the condition for separation, without actually separating.

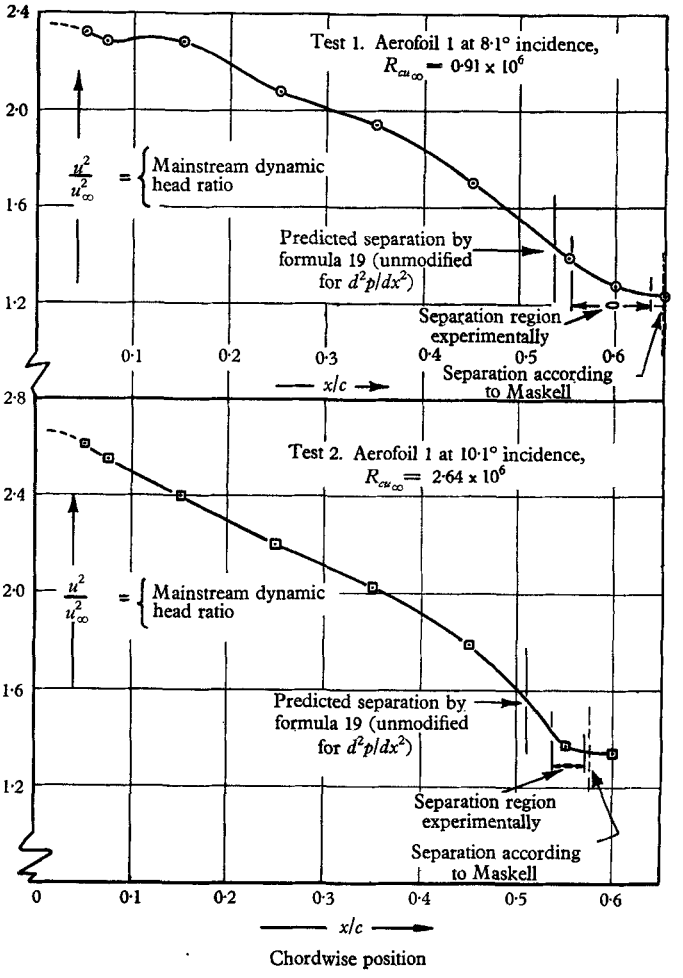

FIGURE 6. Tests (1 and 2) of the method before its development to allow for the effect of d^2p/dx^2.

A closer examination of the results in conjunction with the pressure distribution shows that the error in the formulae increases with increase in the value of d^2p/dx^2 immediately prior to separation. Consideration of the theoretical analysis for the laminar boundary layer (Stratford 1954) shows that this is to be expected, and it would have been found in that case also that the use of the result obtained for flow with continuously zero skin friction would have caused a considerable error. At present, there is insufficient data to make full allowance for d^2p/dx^2 in the case

of the turbulent boundary layer, but a crude modification, that would about halve the error, would be to replace equation (19*b*) by

$$\left.\begin{aligned}\beta &= 0{\cdot}66 \quad (d^2p/dx^2 < 0),\\ \beta &= 0{\cdot}73 \quad (d^2p/dx^2 \geqslant 0),\end{aligned}\right\} \tag{23}$$

the relevant value of d^2p/dx^2 being that immediately prior to separation. The final result is then given by equations (19*a*), (19*c*) and (23). For the Reynolds numbers of the order of 10^6, the form quoted in the Summary is a convenient simplification.

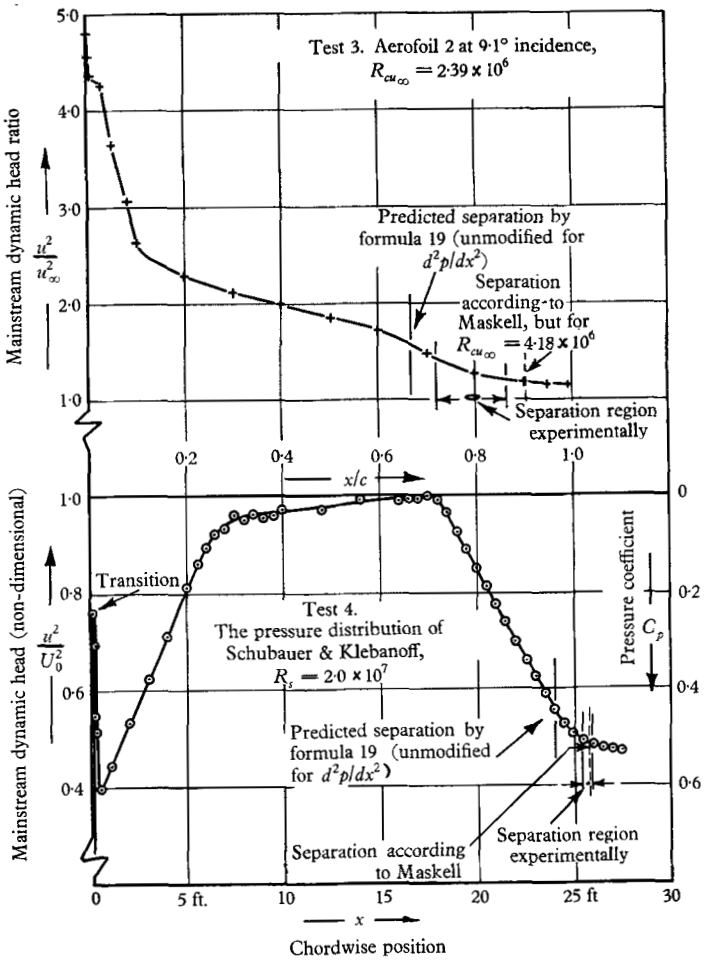

FIGURE 7. Tests (3 and 4) of the method before its development to allow for the effect of d^2p/dx^2.

Further tests would be desirable at extreme Reynolds numbers, in case, for example, the factor β should vary. At present β has been assumed to be independent of the Reynolds number.

As a further test of the basic theoretical concepts the theoretical predictions for the momentum thickness may be compared with the results taken from the experiment with continuously zero skin friction. The predictions are independent

of the empirical factor β when plotted in the form θ_s/θ' against C_p, as in figure 5; it is the more significant therefore that, as may be seen from the figure, the predictions are satisfactorily confirmed. The experiment also confirms the linear dynamic head close to the wall predicted by equations (10) and (14), at least for the special conditions of that experiment where there is no actual reverse flow. With flow reversal the softening of the pressure gradient, together with a new type of turbulence discovered while carrying out the experiment with zero skin friction, might tend to mask the linear dynamic head profile, although the criterion for separation would not be affected.

Test no. ...	1	2	3	4	5
Figure no.	6	6	7	7	4 of next paper
$R_s/10^6$	0·76	2·2	3·4	20	1·0 to 1·6
n (nominal value)	5·9	6·3	6·5	7·3	6·0
$C_{p,s}$ theory, before allowing for $(d^2p/dx^2)_s$	0·372	0·412	0·626	0·442	0 to 0·57, used for empirical fitting
$C_{p,s}$ experiment*	0·409 to 0·470	0·464 to 0·495	0·669 to 0·734	0·460 to 0·530	0 to 0·57, used for empirical fitting
Approx. increase in β required for theory to give agreement with experiment	+8 %	+20 %	+20 %	+2 %	0 %
d^2p/dx^2 immediately prior to separation	Slightly positive	Large and positive	Large and positive	Negative	Maximum negative

* The two experimental values quoted for $C_{p,s}$ for each test, correspond (except in test 5) respectively to the position where $C_p(x\,dC_p/dx)^{\frac{1}{2}}$ is a maximum (this is where the danger of separation is greatest according to the theory), and to the position where dC_p/dx has become zero (due to the separation destroying the pressure rise).

TABLE 1. Tests of the method using equations (19) without correction for $(d^2p/dx^2)_s$

Comparison with other methods

Results of calculations by the method of von Doenhoff & Tetervin (1943) and by that of Maskell (1951) are shown respectively in figure 8, and in figures 6 and 7. von Doenhoff & Tetervin's criterion for separation is that the shape parameter H should lie between 1·8 and 2·6 and this, it will be seen, leaves an indeterminacy of up to about 10 % in the predicted pressure rise to separation, i.e. about the same as for the present method. Maskell improves upon this accuracy mostly by using Ludweig & Tillmann's skin friction law, which, on extrapolation, gives the position of separation once the distributions of H and θ are known. Recently, Spence (1956*a*) has increased the usefulness of these types of analysis by developing a method whereby H may be more rapidly calculated. The accuracy of Maskell's predictions is probably highly satisfactory for most pressure distributions, although difficulty might be experienced with special pressure distributions such as very sharp pressure rises or the flow with continuously zero skin friction.

For most pressure distributions the present method probably would not be as accurate as either Maskell's method or the Maskell–Spence method until the

allowance for d^2p/dx^2 has been improved. However, it should be more accurate than those methods for the special types of pressure distribution mentioned above, and it could be employed generally, taking advantage of its considerably

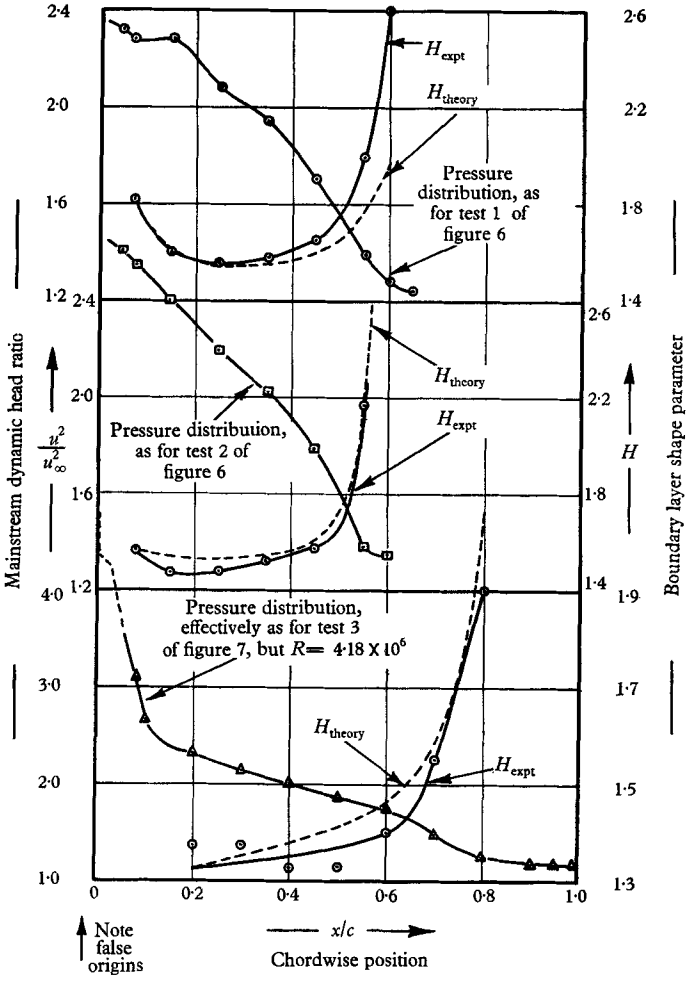

FIGURE 8. Results from the method of von Doenhoff & Tetervin (separation is assumed to occur when H is between 1·8 and 2·6).

greater speed, where its 10 % range of uncertainty is acceptable. Further claims for the present method are that it provides a better physical picture and understanding of the flow, and also a greater flexibility. The latter is demonstrated both by the ease with which may be seen the effects of any change in a given pressure distribution, and by the extension to flow with continuously zero skin friction, as obtained in § 6.

An example

We shall consider the case of a linear pressure rise starting at the leading edge, i.e. $C_p = x/c$. For simplicity it will be assumed that the Reynolds number R_s is

equal to 10^6. Since d^2p/dx^2 is zero, the value 0·73 is used in equation (23); equations (19a) and (19c) (or the equation of the Summary) then become

$$[(x/c)^{\frac{3}{2}}]_s = 0{\cdot}39,$$
$$x_s/c = C_{p,s} = 0{\cdot}53,$$
$$U_s/U_0 = 0{\cdot}68.$$

6. An extension to flow with continuously zero skin friction

If the separation condition of zero skin friction is reached at each point downstream of $x = x_0$, but separation itself is always just avoided, the separation criterion of equations (19) will apply at all positions and consequently will become a differential equation for the pressure distribution. On integration, neglecting the small variation of n with x, the pressure distribution is found to be

$$C_p = 0{\cdot}645\left\{0{\cdot}435R_0^{\frac{1}{6}}\left[\left(\frac{x}{x_0}\right)^{\frac{1}{6}} - 1\right]\right\}^{2/n} \quad \left(\tau_0 \equiv 0,\ C_p \leqslant \frac{n-2}{n+1}\right), \tag{24}$$

where $R_0 = x_0 U_0/\nu$, the coefficient 0·645 being a close fit (to $\frac{1}{2}$% for $6 \leqslant n \leqslant 8$) to a function of n.

At a Reynolds number of $R_0 = 10^6$, when $n \doteqdot 6$, this pressure distribution becomes

$$C_p = 1{\cdot}23\left[\left(\frac{x}{x_0}\right)^{\frac{1}{6}} - 1\right]^{\frac{1}{3}} \quad (\tau_0 \equiv 0,\ C_p \leqslant \tfrac{4}{7}). \tag{25}$$

When $C_p = (n-2)/(n+1)$ the inner layer reaches the edge of the main boundary layer and equation (24) is at the limit of its validity. At greater pressure rises a solution could be sought in which the whole boundary layer retained a constant profile shape. Thus the simple form of the momentum equation is

$$\frac{d}{dx}(\rho U^2\theta) = \tau_0 + \delta^*\frac{dp}{dx}. \tag{26}$$

The value of the shape parameter H, $= \delta^*/\theta$, is put equal to a constant and, with the skin friction τ_0 equal to zero, the equation readily yields

$$\theta = \frac{\text{const.}}{(1-C_p)^{(1+\frac{1}{2}H)}}. \tag{27}$$

This may be transformed into a pressure distribution by direct resort to an argument based on similarity. Alternatively, the inner layer profiles of equations (10), (14) and (15) show that

$$\frac{dp}{dx} \propto \frac{\frac{1}{2}\rho u^2}{y},$$

and therefore, by similarity,

$$\frac{dp}{dx} \propto \frac{\frac{1}{2}\rho U^2}{\theta}. \tag{28}$$

Elimination of θ from equations (27) and (28), integration, and putting $H = 2{\cdot}0$, which would be the value for a linear dynamic head as used in the simplified inner layer profile, leads to

$$C_p = \left[1 - \frac{a}{(x+b)^{\frac{1}{2}}}\right] \quad \left(\tau_0 \equiv 0,\ C_p \geqslant \frac{n-2}{n+1}\right), \tag{29}$$

where a and b are constants, determined by continuity with the pressure distribution of equation (24). For a Reynolds number of $R_0 = 10^6$ continuity with equation (25) gives $a = 0{\cdot}39x_0^{\frac{1}{2}}$ and $b = -0{\cdot}78x_0$.

This extension of the theory has utilized the empirical value $\beta = 0{\cdot}66$ obtained from the experiment with zero skin friction; the closeness of the empirical fitting may be judged from the comparison shown in figure 4 of the following paper.

The work leading to the present paper was started in the Aeronautics Department of Imperial College and has been completed at the National Gas Turbine Establishment. The author is indebted to staff and colleagues who have given valuable criticism and advice, and to the Department of Scientific and Industrial Research for a grant which enabled the work to be initiated.

REFERENCES

VON DOENHOFF, A. E. & TETERVIN, N. 1943 *Rep. Nat. Adv. Comm. Aero., Wash.*, no. 772.

DURAND, W. F. (Ed.) 1943 *Aerodynamic Theory*, Vol. III. California Institute of Technology.

GOLDSTEIN, S. (Ed.) 1938 *Modern Developments in Fluid Dynamics*, Vols. I and II. Oxford University Press.

KALIKHMANN, L. E. 1943 *Dokl. Akad. Nauk, SSSR*, **38**, 165.

LUDWEIG, H. & TILLMANN, W. 1949 *Tech. Mem. Nat. Adv. Comm. Aero., Wash.*, no. 1285 (transl.).

MASKELL, E. C. 1951 *Aero. Res. Coun., Lond.*, Unpublished Paper no. 14, 654.

ROTTA, J. 1953 Rep. no. 8. University of Göttingen.

SCHLICHTING, H. 1941 *Tech. Mem. Nat. Adv. Comm. Aero., Wash.*, no. 1218 (transl.).

SCHUBAUER, G. B. & KLEBANOFF, P. S. 1950 *Rep. Nat. Adv. Comm. Aero., Wash.*, no. 1030.

SPENCE, D. A. 1956*a* *Aero. Res. Coun., Lond.*, Unpublished Paper no. 18,261. (Modified method by Spence; also a review of methods including those of Garner, Schuh, Truckenbrodt, and Zaat.)

SPENCE, D. A. 1956*b* *J. Aero. Sci.* **23**, 3.

SQUIRE, H. B. 1950 *Rep. & Mem. Aero. Res. Coun., Lond.*, no. 2751.

SQUIRE, H. B. & YOUNG, A. D. 1937 *Rep. & Mem. Aero. Res. Coun., Lond.*, no. 1838.

STRATFORD, B. S. 1954 *Rep. & Mem. Aero. Res. Coun., Lond.*, no. 3002.

STRATFORD, B. S. 1956 *Curr. Pap. Aero. Res. Coun., Lond.*, no. 307.

STRATFORD, B. S. 1959 *J. Fluid Mech.* **5**, 17.

THWAITES, B. 1949 *Aero. Quart.* **1**, 245.

WALZ, A. 1943 U & M no. 3060. University of Göttingen.

YOUNG, A. D. & WINTERBOTTOM, N. E. 1940 *Rep. & Mem. Aero. Res. Coun., Lond.*, no. 2400.